Surface Science 678 (2018) 194–200

Contents lists available at ScienceDirect

Surface Science

journal homepage: www.elsevier.com/locate/susc

Steering a cycloaddition reaction via the surface structure

Matthias Koch[a], Marie Gille[b], Stefan Hecht[b], Leonhard Grill[a,c,*]

[a] Fritz-Haber-Institut of the Max-Planck-Society, Faradayweg 4-6, Berlin, Germany
[b] Department of Chemistry & IRIS Adlershof, Humboldt-Universität zu Berlin, Brook-Taylor-Str. 2, Berlin, Germany
[c] Department of Physical Chemistry, University of Graz, Heinrichstrasse 28, Graz 8010, Austria

ARTICLE INFO

Keywords:
Scanning tunneling microscopy
On-surface reactions
Au(100)
Au(111)
On-surface synthesis
Cycloaddition reaction

ABSTRACT

The on-surface reaction of 2,3-dibromoanthracene molecules is studied on two surfaces, Au(100) and Au(111) that differ in their surface reconstructions and thus atomic-scale structure. After deposition intact molecules are observed, which form highly ordered close-packed islands, with preferential adsorption along the corrugation rows of the substrate in the case of Au(100). Heating the sample at 520 K induced Br dissociation and on-surface oligomerization of the thus activated anthracene moieties. While dimers and trimers are formed on Au(111) where they segregate into different molecular islands, only dimers are generated on Au(100). Hence, the reaction mode can be controlled on Au(100) which clearly favors the [2 + 2]cycloaddition product whereas the [2 + 2 + 2] cycloaddition reaction is suppressed. This high selectivity for forming the linear dimer seems to be caused by the adsorption geometry on the reconstructed Au(100) surface.

1. Introduction

Low-dimensional materials are attracting great interest nowadays, due to their high potential in future applications [1–5]. Their precise composition defines not only their electrical and mechanical properties, but can also be used to tune them in a controlled way and for a specific purpose [6–8]. A bottom-up approach for the fabrication of such materials is based on the deposition of small precursor molecules onto a surface, where the growth process takes place. The organic molecules self-assemble spontaneously at appropriate temperatures and form two-dimensional networks, which are only one atomic layer thick. Depending on the molecule-molecule and molecule-surface interactions, these two-dimensional networks are stabilized by weak van-der Waals interaction or even covalent bonds [9]. Especially the formation of strong C–C bonds, realized by connecting molecular building blocks equipped with halogen atoms, received a lot of attention in the last years [10–12]. This on-surface synthesis method is particularly suitable because the final architectures can be precisely tuned via the chemical structure of the initial building blocks. Accordingly, various nanostructures such as porphyrin and fluorene wires [10,13], graphene nanoribbons [14] with different chemical doping [15] or 2D structures [10,16] could be grown, depending on the choice of the precursor molecules.

High control over the chemical composition is of particular interest in the scope of molecular electronics [17], where individual functional units inside an organic device need to be synthesized with atomic precision [18,19]. A step-wise polymerization process has been achieved through specific activation temperatures of the involved molecular building blocks, equipping the precursor molecules with different halogen atoms [16]. Alternatively, the catalytic reactivity of the substrate can be used to influence the activation temperature [20–22]. This additional control is vital for the polymerization of fragile precursor molecules [21]. Beside the activation temperature, also the type of chemical bond formed between the molecular precursors is influenced by the choice of the substrate as the presence of Cu adatoms can lead to the formation of metal-ligand bonds instead of C–C connections [21,22]. In contrast to reversible metal-ligand bonds [23] and to polymerization via boronic acid condensation that can be reversed in the presence of water [24], strong C–C bonds do not support self-healing approaches [25]. Instead the sample temperature and composition as well as the type and flux of the molecular precursor(s) must be controlled to fabricate polymers with utmost control and to suppress unwanted irreversible side reactions [26].

Initially, we were interested in the formation of planar aromatic nanostructures presenting zig-zag edges for superior electronic properties [27,28]. However, instead of using benzene annulation chemistry as in the case of acenes [29] and wider zig-zag graphene nanoribbons [30], we were targeting to connect six-membered benzene units via four-membered cyclobutadiene units, resembling the [N]phenylene family pioneered by the group of Peter Vollhardt [31]. In particular, the linear [N]phenylenes are interesting as their band gap decreases rapidly [32] and thus they have been predicted as molecular wires [33] as well

* Corresponding author at: University of Graz, Department of Physical Chemistry, Heinrichstrasse 28, 5.OG, Graz 8010, Austria.
E-mail address: leonhard.grill@uni-graz.at (L. Grill).

https://doi.org/10.1016/j.susc.2018.05.014
Received 23 February 2018; Received in revised form 30 April 2018; Accepted 23 May 2018
Available online 29 May 2018
0039-6028/

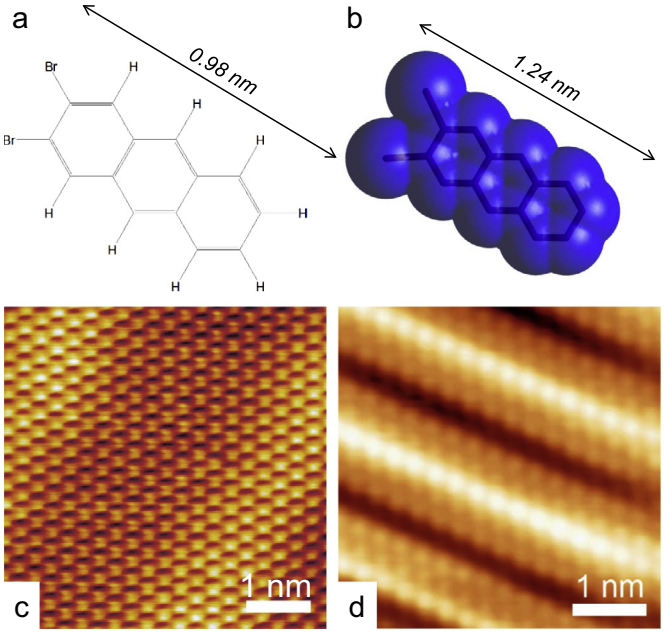

Fig. 1. (a) Chemical sketch of the 2,3-dibromoanthracene (dBA) precursor molecule. The indicated distances between the bromine and hydrogen atom (in a) and the length of the molecule including the van der Waals surface (in b) as determined by the molecular builder software Avogadro 1.2.0, using a MMFF94 force field. STM images of the reconstructed surfaces of Au(111) and Au(100) are shown in c and d, respectively.

as materials for singlet fission [34]. To investigate the feasibility of on-surface synthesis of [N]phenylenes we have used 2,3-dibromoanthracene (dBA, Fig. 1a and b) as the molecular precursor. For the formation of the cyclobutadiene linkage, two carbon-carbon bonds should be formed in an on-surface [2 + 2]cycloaddition reaction, thus transforming two π-bonds into two σ-bonds. In surface chemistry, cycloaddition reactions are of particular importance when organic molecules chemisorb on (001) semiconductor surfaces [35]. In contrast, here we are utilizing this reaction mode to annulate two anthracene moieties on Au(111), which has been used in many on-surface synthesis studies [10,11,14,36]. In order to obtain insight into the role of the substrate on the chemical reaction and the final products, we have employed two different orientations of gold surfaces, Au(111) and Au(100) (Fig. 1c and d).

2. Methods

The high resolution of a scanning tunneling microscope (STM) makes it a suitable tool to investigate the products of chemical reactions on a metallic surface [37]. For imaging the precursor molecules and reaction products on the gold surfaces, we have used a low temperature STM (Createc), operating at 10 K. This instrument is based on the design developed by Gerhard Meyer [38] in the research group of Karl-Heinz Rieder who used it very successfully [39-49], being the second group – after the pioneering work by Don Eigler and co-workers [50] – to show that single atoms can be positioned at will on a surface (i.e. writing letters with single atoms) [51]. The Au(111) and Au(100) surfaces were prepared by multiple cycles of Argon sputtering and annealing at 770 K, resulting in flat surfaces with very few defects. Then, 2,3-dibromoanthracene (dBA) (Fig. 1a) was deposited onto the clean gold surfaces at an evaporation temperature of 400 K while the sample was kept at room temperature. To trigger the polymerization and activation of the molecular precursors the sample was heated at 520 K for one minute before the sample was transferred into the cold STM chamber.

3. Results and discussion

3.1. Surfaces

The clean gold surfaces are both characterized by their reconstructions. In the case of Au(111), this is the so-called herringbone reconstruction, which exhibits a (22 × √3) unit cell as the first atomic layer at the surface is compressed as compared to the atomic positions in the bulk [52]. This results in a surface corrugation of about 20 pm that is visible in STM images as bright stripes (in the upper left and lower right of Fig. 1c) [52]. In the case of the Au(100) surface on the other hand, the surface orientation reveals a quadratic geometry, while the topmost layer of atoms reconstructs in a hexagonal structure. The surface is characterized by a (5 × 20) unit cell [53] and exhibits rows of atoms that protrude from the surface and are clearly visible in STM images (Fig. 1d). These reconstruction rows are typically aligned parallel to step edges on the surface [54] and give rise to a surface corrugation of up to 30 pm [52]. Hence, both samples used in this work exhibit a reconstructed surface with a small corrugation.

3.2. Oligomerization on Au(111)

After deposition of dBA molecules onto the Au(111) surface kept at room temperature, islands are formed (Fig. 2a–d). This observation shows that the molecules are mobile at room temperature since otherwise they would be randomly distributed in a “hit-and-stick” mode. The islands are highly ordered, indicating a close-packing to minimize the intermolecular distances and thus the total energy of the system. The molecules appear very homogeneous apart from two protrusions that are located on the same side of the molecule (Fig. 2d). The low evaporation temperature of the molecules (400 K) makes it unlikely that dehalogenation has already occurred [10,55]. Therefore, we assign these protrusions to bromine atoms which are still attached to the precursor molecules [42]. The length of the molecules is about 1.3 nm (as determined from their width at half maximum intensity in height profiles; see Fig. 2b), in very good agreement with their length in the gas phase where the van der Waals surface has an extension along the molecular symmetry axis of 1.24 nm (Fig. 1b). Accordingly, the molecules seem to be intact, thus not activated yet, and a subsequent annealing step is necessary to cleave the carbon-bromine bond.

At domain boundaries and at edges of these islands individual molecules can be identified that have more degrees of freedom and do not follow the orientation of the self-organized islands (Fig. 2a). However, a closer inspection shows that the individual molecules on Au (111) are all oriented in the same direction. From superimposing single molecules over an STM image of highly ordered areas (Fig. 2c) the molecular arrangement inside an island can be derived (the molecular arrangement is shown enlarged below the STM image). A parallel “head-to-tail” arrangement is found where neighboring molecules are shifted off the molecular axis, probably to minimize their intermolecular distance and thus improve the packing density.

To study the role of the substrate, we deposited the same precursor on Au(100) instead of Au(111). Similar to Au(111), the molecules are mobile at room temperature and they are not activated yet, clearly visible in the non-homogeneous appearance in STM imaging (Fig. 2e–h). The appearance is very similar to the one on Au(111), consisting of a flat rod and protrusions at the end (Fig. 2h). However, in contrast to Au(111), the neighboring molecules self-assemble with their Br substituents facing each other, thus “head-to-head” (Fig. 2g). This adsorption geometry allows a slightly tighter packing of the molecules on Au(100) (with a molecular density of 1.18 ± 0.6 molecules/nm^2) as compared to Au(111) (1.09 ± 0.5 molecules/nm^2).

On Au(100) the molecules typically adsorb parallel to the step edges (as visible in Fig. 2e where an intrinsic step edge of the surface takes course from the upper left to the lower right corner). A height profile across the molecular rows (Fig. 2f) reveals that every second dBA

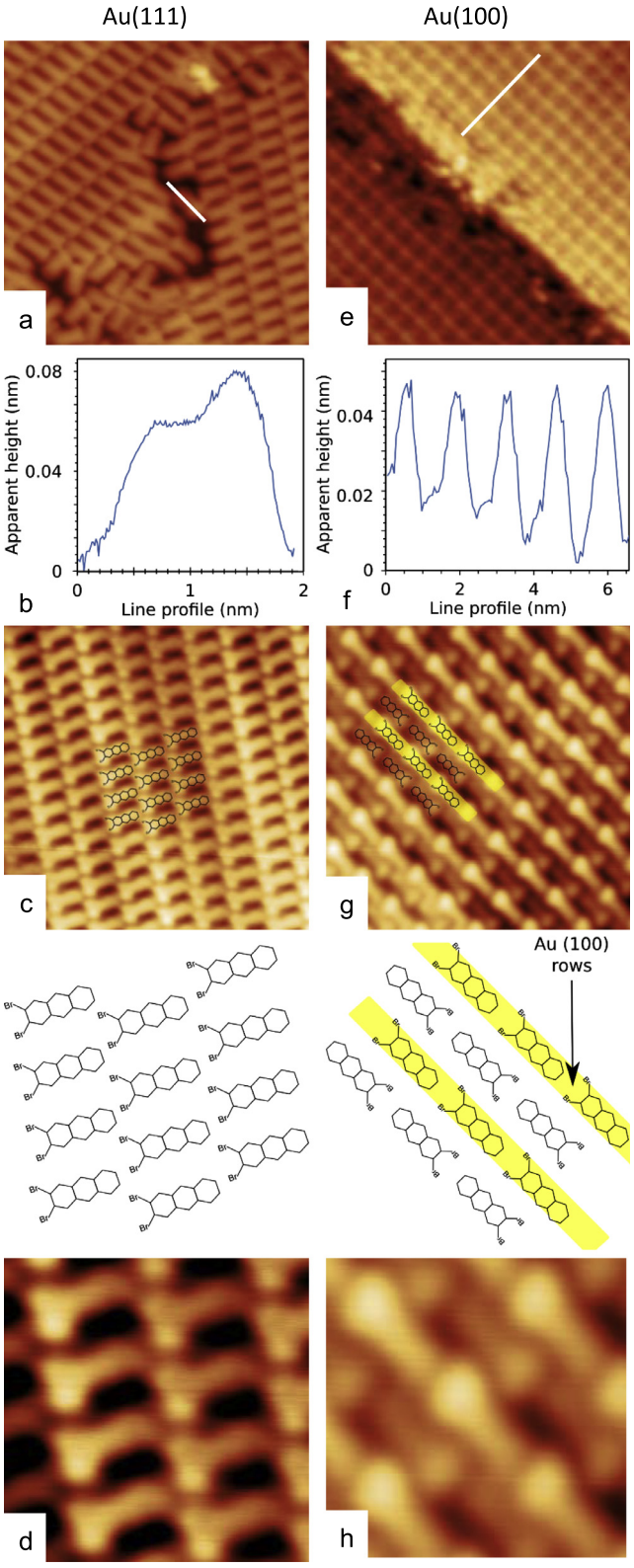

Fig. 2. 2,3-Dibromoanthracene (dBA) molecules on Au(111) (a–d) and Au(100) (e–h). Height profiles across the molecules are plotted in (b) and (f) as indicated in the STM images above. (c and d) and (g and h) show smaller areas of the close-packed dBA islands with schemes of the molecular arrangement. The size of the STM images in (c) and (g) is 10 × 10 nm^2.

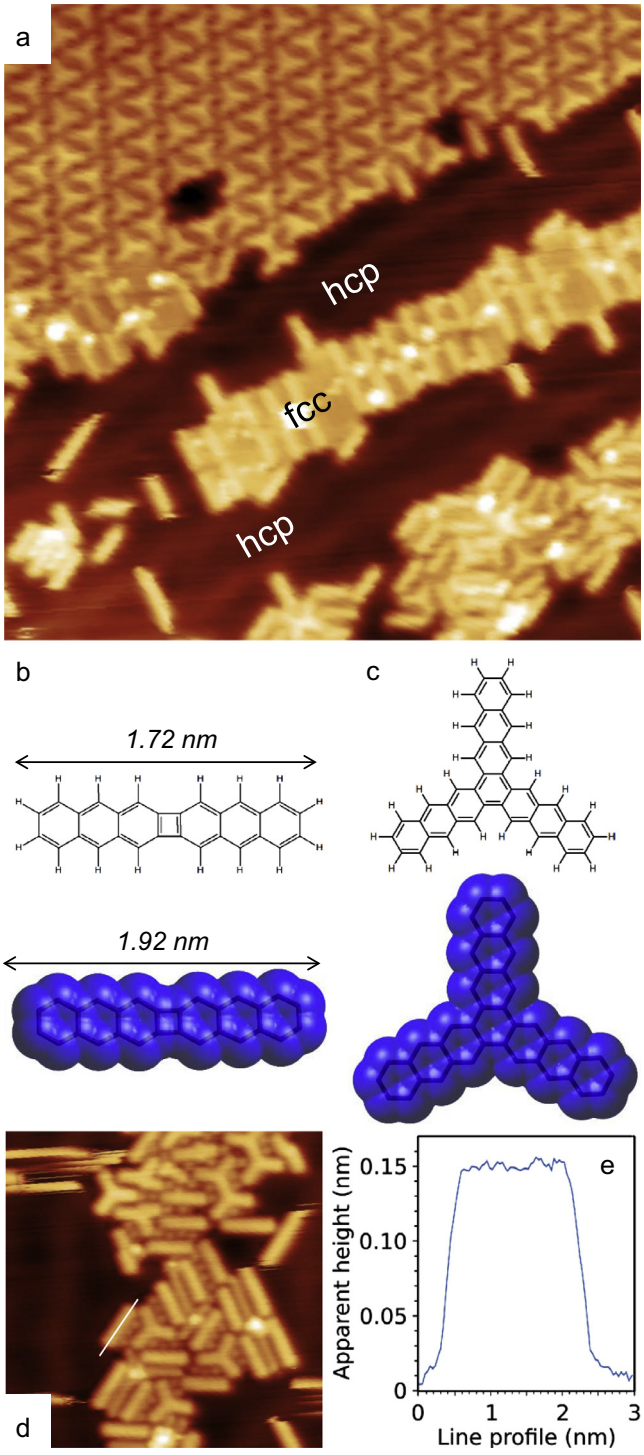

Fig. 3. STM image (30 × 30 nm^2) of 2,3-dibromoanthracene (dBA) on Au(111) after annealing the sample at 470 K, revealing two products of the dBA precursor molecules. The chemical structures of these dimers and trimers are shown in (b and c), including the van der Waals surface (in blue) below. The indicated lengths of a dimer in (b) were determined by the molecular builder software Avogadro 1.2.0 (using a MMFF94 force field) and reflect the distance between the terminal hydrogen atoms (upper panel) and the edges of the van der Waals surface along the dimer molecule (lower panel). (d) STM image (12 × 12 nm^2) of a disordered island with dimers and trimers and (e) corresponding height profile of a dimer molecule.

molecule appears higher in STM imaging, which is even more evident in zoom-in images (Fig. 2g and h). The distance between two higher molecules is found to be 1.35 ± 0.06 nm, which matches exactly the distance between two corrugation rows of the Au(100) reconstruction (1.35 ± 0.04 nm [56]), which run parallel to the step edges. We therefore conclude that every second row of molecules appears brighter, i.e. at a larger apparent height, in STM images because it is located on top of a Au(100) corrugation row while the other molecules are adsorbed in the troughs between, thus at lower height. The molecular packing on the surface is therefore (in the direction perpendicular to the corrugation rows) commensurate with the Au(100) reconstruction underneath, with two molecules within one period of the surface corrugation.

Annealing the Au(111) surface at 520 K leads to very different structures on the surface. In particular, the brighter intramolecular features assigned to the bromines are no longer observed in STM images and the molecular compounds appear with homogeneous heights in STM images (see Fig. 3a and d). Hence, the thermal treatment causes Br dissociation from the molecules, i.e. activates the dBA molecules, and triggers an on-surface reaction. Two different products are formed on the surface: a linear and a star shaped nanostructure (Fig. 3a–c). The linear molecules appear very similar to the intact dBA molecules, i.e. before activation, but lack the two protrusions at the termini, according to the Br dissociation. However, while the length of the intact dBA molecule is approximately 1.3 nm (see above), the linear structures are about 2.0 nm long (Fig. 3d and e), thus indicating a larger molecule. In particular, this value is in very good agreement with gas phase calculations (using a MMFF94 force field with the *Avogadro* software), which find the dimer to be 1.92 nm long (Fig. 3b). Note, that we do not find other linear products (shorter or longer) which points to a very well-defined reaction.

We suggest that the linear structures are dimers that exhibit the chemical structure shown in Fig. 3b. They are very smooth and flat in STM images with an apparent height of about 0.13 nm. This is on the one hand similar to graphene nanoribbons where on the same, Au(111), surface apparent heights of about 0.15 nm have been reported [57]. On the other hand, the overall appearance of the molecules is very similar to tetracene dimers that were formed by the on-surface covalent linking of 2,3-dibromotetracene [58]. Since the precursor is very similar to the molecules used in the present work, only differing by an additional benzene ring, also the same type of covalent linking can be expected. No other linear products (of shorter or longer dimensions) have been found there [58], in agreement with our observations. These similarities allow assignment of the molecules observed on the surface to the dimer structure given in Fig. 3b. Note that four-membered carbon-based rings can be thermodynamically stable, in particular if conjugated and fused to six-membered benzene moieties, as is the case here. The resulting compound family of the so-called [N]phenylenes includes many linear, bent, and branched derivatives [31,32].

The second product we observe after annealing the Au(111) surface at 520 K is a star-shaped trimer with three dBA arms rotated by 120° (upper half of Fig. 3a and c). Both products – linear dimers and triangular trimers – self-assemble when cooling the sample to low-temperature in large molecular islands. However, these arrays consist predominantly either of dimer or trimer molecules (Fig. 4). In each of them the molecules close-pack and from their characteristic appearance the high molecular order can be determined (Fig. 4b and d). Hence, the molecular nanostructures produced in the thermal treatment segregate on the surface, probably for energetic reasons since packing would be less efficient in a heterogeneous island that require more space, as visible in Fig. 3d. However, although rather rare, the close-packing is not perfect on the surface and in some cases disordered islands appear that contain a mixture of different products, for instance at the upper right of Fig. 3d. Based on the dimensions of these two dumbbell shaped molecules they are presumably anthracene pentamers, in which the central anthracene unit is connected on both of its termini to a benzene

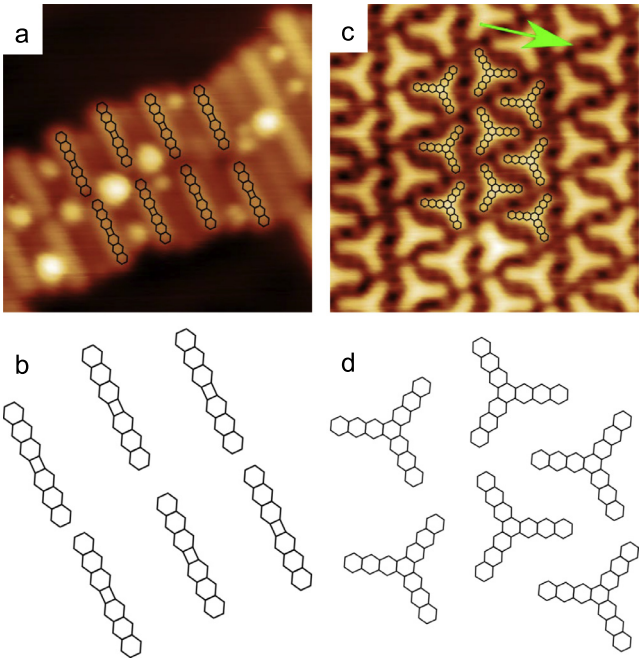

Fig. 4. (a) After annealing the Au(111) surface to 520 K two products are observed. The chemical structure (without H atoms for the sake of better visibility) and STM images are shown in (b, c) for linear di-anthracene (10 × 10 nm^2) and in (c,e) for triangular tri-anthracene (5 × 5 nm^2). A protrusion that we assign to be a bromine atom is indicated by the arrow in (c).

branchpoint as observed in the more abundant trimers.

Between the trimers within their close-packed islands, lobes of smaller apparent height appear (see green arrow in Fig. 4c). They are very characteristic and since they are only found after activation of the molecules, we attribute them to individual bromine atoms [59]. While the trimers cover all areas of the Au(111) surface equivalently, the dimers prefer to adsorb on the wider fcc regions of the Au(111) surface. This is visible in STM images that show clean hcp regions next to dimer islands adsorbed in a roughly linear fashion along the fcc areas (in the center of Fig. 3a) while in the same area (upper left of Fig. 3a) the trimer island is not influenced by the herringbone reconstruction underneath. Such an effect of preferential molecular adsorption on the fcc areas of the reconstructed Au(111) surface has been observed for 1-nitronaphtalene molecules that adsorb at step edges [60].

From these observations we conclude that two competing reactions occur during the oligomerization process on Au(111): A [2 + 2]cycloaddition leading to formation of the linear dimer and a [2 + 2 + 2] cycloaddition giving rise to formation of the triangular trimers. The relative efficiency of the [2 + 2] and [2 + 2 + 2] cycloaddition reactions, i.e. the so called periselectivity, on Au(111) can be evaluated by counting 1311 dimer and trimer products on the surface. We find a distribution of 46% dimers and 54% trimers, indicating that both pathways have about equal probability. This is in good agreement with calculations performed for 2,3-dibromotetracene on Ag(111) (i.e. also an acene, but with an additional benzene ring), which find similar energy barriers for the formation of dimer and trimer products [58]. From our observables, we can only speculate about the actual mechanism of the reaction, which clearly needs to be initiated by cleavage of the carbon-bromine bond. Presumably, two-fold cleavage leads to formation of the *ortho*-diradical, which resembles the mesomeric structure of an aryne that subsequently undergoes either [2 + 2] or [2 + 2 + 2]cycloaddition. While the latter mode has been extensively explored in the synthesis of triphenylene and related annulated oligobenzenoid structures [61], the [2 + 2]cycloaddition mode is typically not observed in solution as it is formally forbidden according to the Woodward-Hoffmann rules [62], which predict a high thermal barrier

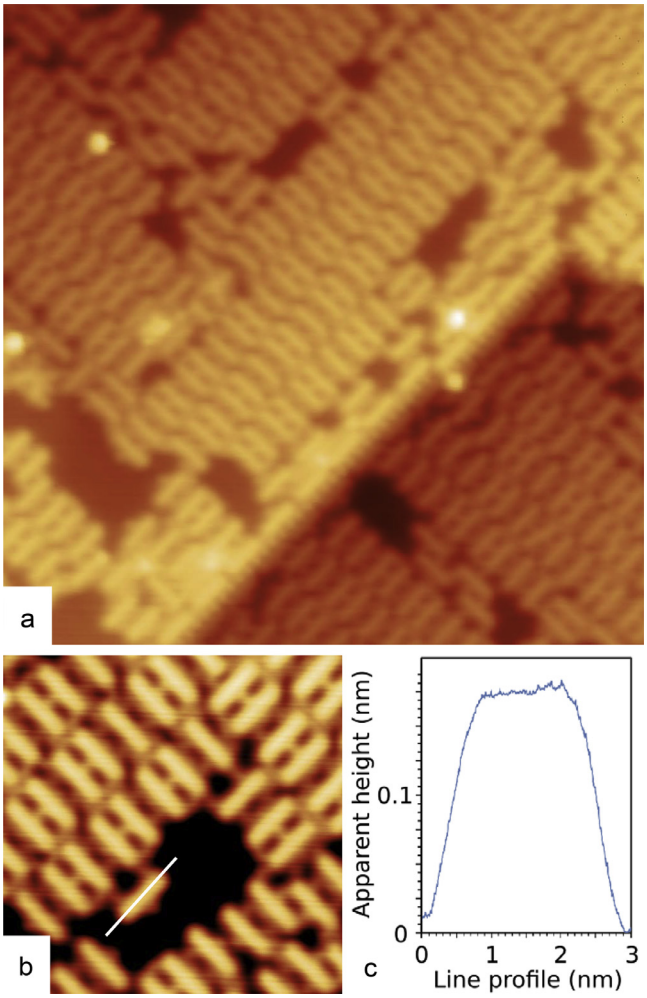

Fig. 5. (a) 2,3-dibromoanthracene (dBA) deposited on Au(100) after annealing the surface at 520 K (30 × 30 nm^2). (b,c) STM image (10 × 10 nm^2) and corresponding height profile of an individual molecule dimer.

for this reaction.

3.3. Oligomerization on Au(100)

Next, we changed the surface – not in its material but in its orientation – and investigated the same polymerization reaction, i.e. depositing identical precursor molecules and heating the sample afterwards. Also on Au(100) the dBA precursor molecules are activated after annealing the surface to 520 K (the initial surface after molecule deposition, but before heating, is shown in Fig. 2e–h). STM imaging shows almost exclusively polymerized dimers on the surface (Fig. 5). The dimers are decorated with bromine atoms between the molecules and appear identical to those found on the Au(111) surface, based on three properties: First their shape, second their flat appearance and third their length of about 2.0 nm (in good agreement with the gas phase dimensions of the dimers, see Fig. 3b).

However, there is a fundamental difference to the Au(111) surface as we do not find any trimers on the Au(100) surface. In view of very recent calculations predicting a comparable energy barrier for the formation of dimers and trimers from the similar and only slightly elongated 2,3-dibromotetracene on Ag(111) [58], the remarkable selectivity observed is somewhat surprising. Additionally, both barriers are lower than the activation (dehalogenation) barrier of the precursor molecule [58]. Hence, as soon as activation takes place, it could be expected that also trimer formation sets in. Nevertheless, we find that the cycloaddition reaction is extremely selective on Au(100) and clearly favors the [2 + 2]cycloaddition product and assign this to the surface morphology, due to the presence of trimers on Au(111).

We explain this high selectivity with the starting product for the formation of a trimer, which requires that the first two connected anthracene arms are oriented non-parallel to one another (shown schematically at the right of Fig. 6c). Furthermore, parallel alignment is the energetically most efficient reaction geometry for dimer formation of the very similar 2,3-dibromotetracene molecules [58]. Here, it should be noted that the adsorption geometry of monomers, i.e. precursor molecules, inside the close-packed islands differs for the two surfaces, Au(111) and Au(100), most likely due to the surface reconstruction as discussed above. These patterns are shown at the bottom of Fig. 2c and g. Similarly, the Au(100) reconstruction could explain the exclusive formation of dimers as evident from large-scale images before the sample heating. While dBA molecules adsorb on Au(111) roughly perpendicular with respect to the corrugation from the herringbone reconstruction (Fig. 6b), they follow the surface reconstruction on Au (100) and align strictly parallel to the corrugation rows (Fig. 6a and at the left in Fig. 6c). Hence, they exhibit a clear pre-orientation at low temperatures before inducing the surface reaction. This could indicate that on Au(100) adsorption of dBA molecules perpendicular to the corrugation rows is energetically disfavored, even at relatively high temperatures that are used during sample heating. At elevated temperatures, the high coverage might even promote a parallel alignment of the molecules with respect to the corrugation. This could be of particular importance for the formation of trimers because they require linking of three molecules that are not parallel, but rotated by ± 120° with respect to each other. In other words: one dBA arm must be perpendicular to the corrugation rows, which are separated by 1.44 nm (as sketched at the right of Fig. 6c). If this adsorption geometry is suppressed on Au(100), trimers cannot form and only dimers are observed, in agreement with our experimental findings.

Another possible explanation comes from the adsorption geometry of the precursor molecules on the surface, prior to polymerization. On both surfaces the molecules adsorb in a parallel arrangement. However, while on Au(111) the molecules do not form rows but neighboring molecules are slightly displaced sideways (Fig. 2c), on Au(100) the molecules are forced by the surface reconstruction to form a precise head-to-tail arrangement in lines (Fig. 2g with the reconstruction sketched in yellow). Note that it has been shown by nudged elastic band (NEB) calculations for the similar 2,3-dibromotetracene molecules on the flat Ag(111) surface that such a rather small difference of the molecular arrangement can substantially modify the energy landscapes along the reaction pathways for dimerization [58]. This pre-arrangement in close-packed layers could then become important when the reaction sets in since neighboring molecules within one reconstruction row (i.e. the molecules between two parallel yellow stripes in Fig. 2g) are exactly in place for dimerization. Hence, it might be argued that dimerization is more efficient on the Au(100) surface than the formation of trimers that are consequently absent after the heating procedure.

It is important to note that the molecular coverage probably plays an important role in this process since we have used rather high coverages of almost one monolayer where the molecules have limited degrees of freedom and are kept in close-packed structures, perhaps even at higher temperatures. On the other hand, more isolated molecules could diffuse over the surface at small coverages where the close-packing constraint is absent. Thus, molecular rotations could be more likely on the Au(100) surface and consequently trimers might be present.

4. Conclusions

We have shown that dBA oligomerizes after activation at 520 K on Au(111) and Au(100), with different results. On Au(111) both [2 + 2] cycloaddition and [2 + 2 + 2]cycloaddition reactions occur and the

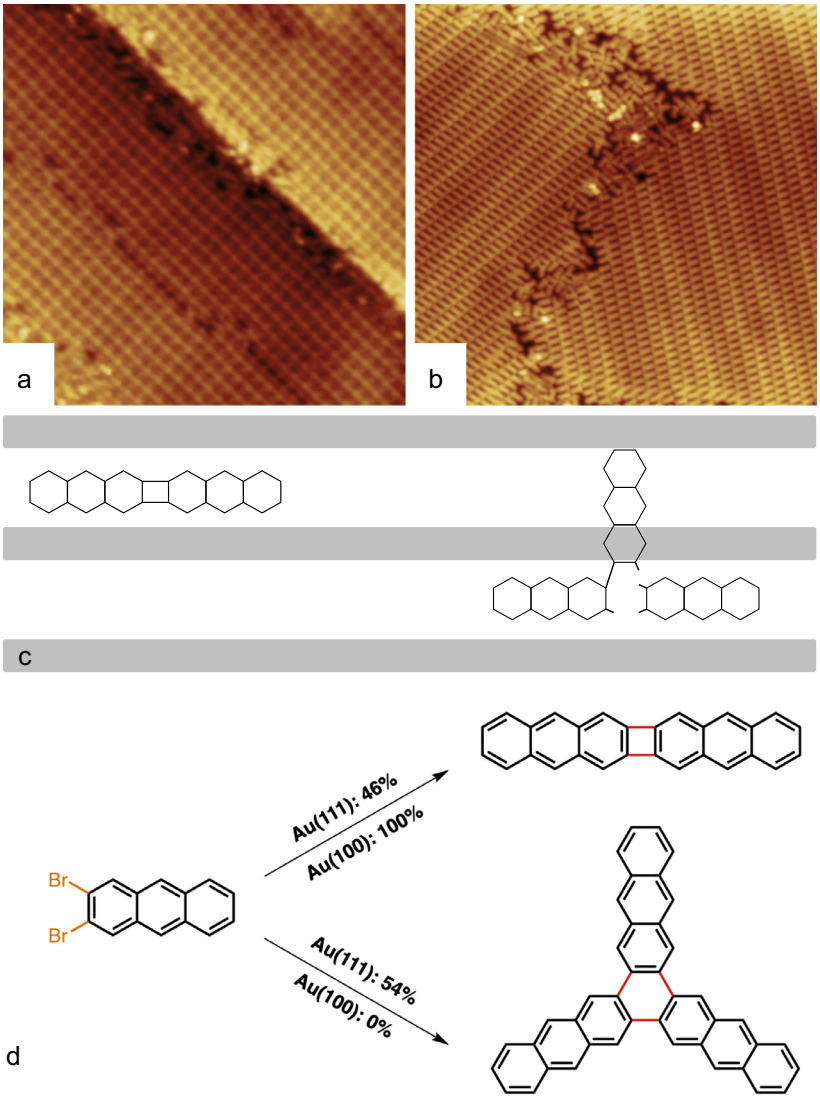

Fig. 6. (a,b) STM images of dBA on Au(100) and Au(111) (37 × 37 nm^2), respectively. STM images of smaller areas are presented in Fig. 2. (c) Sketch of the possible polymerization process on Au(100) with the reconstruction rows of the substrate shown as grey horizontal stripes. (d) Overview of the chemical reactions occurring on Au(111) and Au(100).

formation of about equal amounts of linear dimers as well as star-shaped trimers is observed. In contrast, on Au(100) only linear dimers are formed during the oligomerization step. Our results show that the cycloaddition reaction mode (periselectivity) can be controlled by the choice of the substrate, which clearly has a strong influence on the final reaction product (as sketched in Fig. 6d). We tentatively assign this effect to the corrugation of the Au(100) surface which supports the parallel alignment of the precursor molecules in an ideal arrangement for dimerization, thereby effectively enhancing this process in comparison to trimer formation.

References

[1] J. Sakamoto, J. v. Heijst, O. Lukin, A.D. Schlüter, Angew. Chem. Int. Ed. 48 (2009) 1030.
[2] R. Mas-Balleste, C. Gomez-Navarro, J. Gomez-Herrero, F. Zamora, Nanoscale 3 (2011) 20.
[3] A.K. Geim, I.V. Grigorieva, Nature 499 (2013) 419.
[4] M. Naguib, V.N. Mochalin, M.W. Barsoum, Y. Gogotsi, Adv. Mater. 26 (2014) 992.
[5] K.S. Novoselov, A. Mishchenko, A. Carvalho, A.H.C. Neto, Nature 353 (2016) 461.
[6] M.S. Dresselhaus, G. Chen, M.Y. Tang, R. Yang, H. Lee, D. Wang, Z. Ren, J.-P. Fleurial, P. Gogna, Adv. Mater. 19 (2007) 1043.
[7] A.A. Balandin, D.L. Nika, Mater. Today 15 (2012) 266.
[8] Q. Tang, Z. Zhou, Progr. Mater. Sci. 58 (2013) 1244.
[9] A. Kühnle, Curr. Opin. Colloid Interface Sci. 14 (2009) 157.
[10] L. Grill, M. Dyer, L. Lafferentz, M. Persson, M.V. Peters, S. Hecht, Nat. Nanotech. 2 (2007) 687.
[11] J. Mendez, M.F. Lopez, J.A. Martin-Gago, Chem. Sov. Rev. 40 (2011) 4578.
[12] L. Talirz, P. Ruffieux, R. Fasel, Adv. Mater. 28 (2016) 6222.
[13] L. Lafferentz, F. Ample, H. Yu, S. Hecht, C. Joachim, L. Grill, Science 323 (2009) 1193.
[14] J. Cai, P. Ruffieux, R. Jaafar, M. Bieri, T. Braun, S. Blankenburg, M. Muoth, A.P. Seitsonen, M. Saleh, X. Feng, K. Müllen, R. Fasel, Nature 466 (2010) 470.
[15] S. Kawai, S. Saito, S. Osumi, S. Yamaguchi, A.S. Foster, P. Spijker, E. Meyer, Nature Commun. 6 (2015) 8098.
[16] L. Lafferentz, V. Eberhardt, C. Dri, C. Africh, G. Comelli, F. Esch, S. Hecht, L. Grill, Nature Chem. 4 (2012) 215.
[17] A. Aviram, M. Ratner, Chem. Phys. Lett. 29 (1974) 277.
[18] J.M. Tour, Acc. Chem. Res. 33 (2000) 791.
[19] T.A. Su, M. Neupane, M.L. Steigerwald, L. Venkataraman, C. Nuckolls, Nat. Rev. Mater. 1 (2016) 16002.
[20] M. Bieri, M.-T. Nguyen, O. Gröning, J. Cai, M. Treier, K. Ait-Mansour, P. Ruffieux, C.A. Pignedoli, D. Passerone, M. Kastler, K. Müllen, R. Fasel, J. Am. Chem. Soc. 132 (2010) 16669.
[21] C.J. Villagomez, T. Sasaki, J.M. Tour, L. Grill, J. Am. Chem. Soc. 132 (2010) 16848.
[22] M. Koch, M. Gille, A. Viertel, S. Hecht, L. Grill, Surf. Sci. 627 (2014) 70.
[23] R. Ohmann, L. Vitali, K. Kern, Nano Lett. 10 (2010) 2995.
[24] J.F. Dienstmaier, A. Gigler, A.J. Goetz, P. Knochel, T. Bein, A. Lyapin, S. Reichlmaier, W.M. Heckl, M. Lackinger, ACS Nano 5 (2011) 9737.
[25] J. Eichhorn, T. Strunskus, A. Rastgoo-Lahrood, D. Samanta, M. Schmittel, M. Lackinger, Chem. Commun. 50 (2014) 7680.
[26] J. Eichhorn, D. Nieckarz, O. Ochs, D. Samanta, M. Schmittel, P.J. Szabelski,

M. Lackinger, ACS Nano 8 (2014) 7880.
[27] I. Tamm, Phys. Z. Sowjetunion 1 (1932) 733.
[28] M. Koch, F. Ample, C. Joachim, L. Grill, Nat. Nanotech. 7 (2012) 713.
[29] J.E. Anthony, Angew. Chem. Int. Ed. 47 (2008) 452.
[30] P. Ruffieux, S. Wang, B. Yang, C. Sanchez-Sanchez, J. Liu, T. Dienel, L. Talirz, P. Shinde, C.A. Pignedoli, D. Passerone, T. Dumslaff, X. Feng, K. Müllen, R. Fasel, Nature 531 (2016) 489.
[31] O.S. Miljanic and K.P.C. Vollhardt, Carbon-rich compounds: from molecules to materials (M. M. Haley, R. R. Tykwinski, Eds.; Wiley-VCH Weinheim) (2006) 140.
[32] C. Dosche, H.-G. Löhmannsröben, A. Bieser, P.I. Dosa, S. Han, M. Iwamoto, A. Schleifenbaum, K.P.C. Vollhardt, Phys. Chem. Chem. Phys. 4 (2002) 2156.
[33] N. Trinajstic, T.G. Schmalz, S. Nikolic, G.E. Hite, D.J. Klein, W.A. Seitz, New J. Chem. 15 (1991) 27.
[34] M.B. Smith, J. Michl, Chem. Rev. 110 (2010) 6891.
[35] R.J. Hamers, S.K. Coulter, M.D. Ellison, J.S. Hovis, D.F. Padowitz, M.P. Schwartz, C.M. Greenlief, J.N. Russell, Acc. Chem. Res. 33 (2000) 617.
[36] S. Weigelt, C. Busse, C. Bombis, M.M. Knudsen, K.V. Gothelf, T. Strunskus, C. Wöll, M. Dahlbom, B. Hammer, E. Laegsgaard, F. Besenbacher, T.R. Linderoth, Angew. Chem. Int. Ed. 46 (2007) 9227.
[37] A.-A. Dhirani, R.W. Zehner, R.P. Hsung, P. Guyot-Sionnest, L.R. Sita, J. Am. Chem. Soc. 118 (1996) 3319.
[38] G. Meyer, Rev. Sci. Instrum. 67 (1996) 2960.
[39] G. Meyer, K.-H. Rieder, Surf. Sci. 377-379 (1996) 1087.
[40] L. Bartels, G. Meyer, K.-H. Rieder, Phys. Rev. Lett. 79 (1997) 697.
[41] G. Meyer, J. Repp, S. Zöphel, K.-F. Braun, S.W. Hla, S. Fölsch, L. Bartels, F. Moresco, K.-H. Rieder, Single Molecules 1 (2000) 79.
[42] S.-W. Hla, L. Bartels, G. Meyer, K.-H. Rieder, Phys. Rev. Lett. 85 (2000) 2777.
[43] J. Repp, F. Moresco, G. Meyer, K.-H. Rieder, P. Hyldgaard, M. Persson, Phys. Rev. Lett. 85 (2000) 2981.
[44] F. Moresco, G. Meyer, K.-H. Rieder, H. Tang, A. Gourdon, C. Joachim, Phys. Rev. Lett. 86 (2001) 672.
[45] K.-H. Rieder, G. Meyer, S.-W. Hla, F. Moresco, K.F. Braun, K. Morgenstern, J. Repp, S. Foelsch, L. Bartels, Phil. Trans. R. Soc. Lond. A 362 (2004) 1207.
[46] K.-H. Rieder, G. Meyer, F. Moresco, K. Morgenstern, S.-W. Hla, J. Repp, M. Alemani, L. Grill, L. Gross, M. Mehlhorn, H. Gawronski, V. Simic-Milosevich, J. Henzl, K.F. Braun, S. Foelsch, L. Bartels, J. Phys.: Conf. Ser. 19 (2005) 175.
[47] L. Gross, K.-H. Rieder, F. Moresco, S.M. Stojkovic, A. Gourdon, C. Joachim, Nature Mater. 4 (2005) 892.
[48] L. Grill, K.-H. Rieder, F. Moresco, G. Rapenne, S. Stojkovic, X. Bouju, C. Joachim, Nat. Nanotech. 2 (2007) 95.
[49] K. Morgenstern, N. Lorente, K.-H. Rieder, Phys. Status Solidi B 250 (2013) 1671.
[50] D.M. Eigler, E.K. Schweizer, Nature 344 (1990) 524.
[51] G. Meyer, B. Neu, K.-H. Rieder, Appl. Phys. A 60 (1995) 343.
[52] J.V. Barth, H. Brune, G. Ertl, R.J. Behm, Phys. Rev. B 42 (1990) 9307.
[53] P. Havu, V. Blum, V. Havu, P. Rinke, M. Scheffler, Phys. Rev. B 82 (2010) 161418.
[54] N. Batina, A.S. Dakkouri, D.M. Kolb, J. Electroanal. Chem. 370 (1994) 87.
[55] S.A. Krasnikov, C.M. Doyle, N.N. Sergeeva, A.B. Preobrajenski, N.A. Vinogradov, Y.N. Sergeeva, A.A. Zakharov, M.O. Senge, A.A. Cafolla, Nano Res. 4 (2011) 376.
[56] C.D. Tempas, D. Skomski, S.L. Tait, Surf. Sci. 654 (2016) 33.
[57] P. Ruffieux, J. Cai, N.C. Plumb, L. Patthey, D. Prezzi, A. Ferretti, E. Molinari, X. Feng, K. Müllen, C.A. Pignedoli, R. Fasel, ACS Nano 6 (2012) 6930.
[58] C. Sanchez-Sanchez, A. Nicolai, F. Rossel, J. Cai, J. Liu, X. Feng, K. Müllen, P. Ruffieux, R. Fasel, V. Meunier, J. Am. Chem. Soc. 139 (2017) 17617.
[59] J.A. Lipton-Duffin, O. Ivasenko, D.F. Perepichka, F. Rosei, Small 5 (2009) 592.
[60] M. Vladimirova, M. Stengel, A.D. Vita, A. Baldereschi, M. Böhringer, K. Morgenstern, R. Berndt, W.-D. Schneider, Europhys. Lett. 56 (2001) 254.
[61] D. Perez, D. Pena, E. Guitian, Eur. J. Org. Chem. (2013) 5981.
[62] R.B. Woodward, R. Hoffmann, Angew. Chem. Int. Ed. 8 (1969) 781.